Journal of Molecular Liquids 196 (2014) 238–243

Contents lists available at ScienceDirect

Journal of Molecular Liquids

journal homepage: www.elsevier.com/locate/molliq

Core–shell octa(azidopropyl) POSS–PEO micelle via “click” chemistry

Yujing Li, Liqiang Wan, Farong Huang *, Lei Du

Key Laboratory for Specially Functional Polymeric Materials and Related Technology of the Ministry of Education, School of Materials Science and Engineering, East China University of Science and Technology, Shanghai 200237, PR China

A R T I C L E I N F O

Article history:
Received 27 August 2013
Received in revised form 8 February 2014
Accepted 30 March 2014
Available online 13 April 2014

Keywords:
Octa(azidopropyl) POSS
Propargyl-terminated PEO
Micelle
Core–shell

A B S T R A C T

An amphiphilic OAPS–PEO was synthesized by “click” reaction between octa(azidopropyl) POSS (OAPS) and propargyl-terminated PEO. The structure of OAPS–PEO was characterized by nuclear magnetic resonance (NMR). The amphiphilic properties and aggregation process of OAPS–PEO in aqueous solution were investigated by fluorescence, dynamic and static light scattering (DLS and SLS), and transmission electron microscopy (TEM). The critical aggregates concentration was determined at ~0.10 mg/mL using fluorescence measurements. At this concentration, unassociated unimolecular micelles with diameter size of 40–50 nm were found by DLS, and were also studied by means of TEM. At a lower concentration, all the OAPS–PEO self-assembled into loose balls. With the increase of the OAPS–PEO polymer concentration, OAPS centralizes to be the core of the aggregates. At the concentration of 2.0 mg/mL, aggregates present to be a core–shell structure.

© 2014 Elsevier B.V. All rights reserved.

1. Introduction

Cage-like silsesquioxanes are usually called as polyhedral oligomeric silsesquioxanes (POSSs) which have attracted a great deal of attention in material fields because of their unique nanoscale cage-shaped structures and an interesting properties [1–4]. Their structures feature well-defined and highly symmetric molecules with cubic inorganic core having the size of ~1.5 nm in diameter, while including R groups positioned at the silicon–oxygen cage vertex [5]. R groups (organic shell) can be varied from hydrogen to alkyl (methyl, isobutyl, cyclopentyl or cyclohexyl, etc.), alkylene, or arylene. The POSS molecules with the composition of $R_8Si_8O_{12}$ or $R_1R_7Si_8O_{12}$ are the most studied systems. Thus, POSS molecules can be regarded as truly inorganic core/organic shell architectures, which are compatible with polymers and natural biomaterials. $R_8Si_8O_{12}$ with eight reactionable R groups can be easily regarded as a core of 3-dimension grafting polymer. As we know, poly (ethylene oxide) (PEO) is a highly water-soluble polymer with remarkable properties, such as biocompatibility and nontoxicity. The grafting of PEO onto POSS could largely increase the solubility of POSS molecules, and produce an amphiphile.

R. Knischka et al. [6] reported the synthesis and the characterization of monosubstituted POSS, 1-(1,ω-propylenemethoxy) oligo (ethylene oxide)-3,4,7,9,11, 13,15-heptahydridopentacyclo octasiloxane. They used H_2PtCl_6 to catalyze the Si–H and ethylene to graft PEO onto POSS. Aggregation of the uncondensed amphiphile leads to micelle and vesicular structures that can be cross-linked to liposome-like silica particles at elevated pH. Prithwiraj Maitra et al. [7] used $(HSiMe_2O)_8Si_8O_{12}$ reacted with allyl-PEO to increase ionic conductivity of PEO. The reaction is also between Si–H and ethylene of $(HSiMe_2O)_8Si_8O_{12}$ and allyl-PEO. And other linkage between POSS and PEO like $HN-C=O$ was also reported [8]. “Click” reaction between azide and alkyne which has advantages of high yield, mild reaction conditions, absence of by-products, excellent selectivity and tolerance to a wide range of functionalities can smoothly form a stable 1,2,3-triazole linkage [9,10]. Many reports have widely used this reaction for constructing diverse molecular structures. Zhishen Ge et al. [11] reported quatrefoil-shaped star-cyclic polymer containing a POSS core which was synthesized by “click” reaction. It was substantiated that approximately 7–8 arms of PS (polystyrene) were attached with POSS core. It is undoubted that “click” reaction is a more efficient way to graft arms onto POSS core.

To our knowledge, although the aqueous solution properties and aggregation behavior of the amphiphilic multiarm POSS–PEO have been previously reported [6,12], and the number of the substituent is always less than eight. One of the reasons is the steric hindrance of high molecular weight PEO, the other is that the reaction between core and arms is not very efficient. Here, we apply “click” reaction in the preparation of it.

Octa (azidopropyl) POSS (OAPS) which has eight N_3 groups as the core of amphiphilic polymer can easily react with $HC\equiv C-$ groups. The long chain PEO linked with POSS through triazole rings efficiently. The physical properties and the aggregation behavior of amphiphilic multiarm OAPS–PEO in aqueous solution were investigated.

---

* Corresponding author at: Key Laboratory for Specially Functional Polymeric Materials and Related Technology of the Ministry of Education, School of Materials Science and Engineering, 4 East China University of Science and Technology, Shanghai 200237, PR China. Tel.: +86 21 64251110; fax: +86 21 64251087.
E-mail address: fhuanglab@ecust.edu.cn (F. Huang).

http://dx.doi.org/10.1016/j.molliq.2014.03.047
0167-7322/© 2014 Elsevier B.V. All rights reserved.

2. Experimental

2.1. Materials

Methoxypolyethylene glycols and 3-chloropropyltris(trimethylsiloxy) silane were purchased from Aladdin Industrial Corporation and Pansine Chemical Co., Ltd., respectively. The dialysis bag (Membra-cel, 3500 molecular weight cut-off) was provided by Serva Electrophoresis GmbH. Analytical-grade tetrahydrofuran (THF) was refluxed with sodium and distilled immediately before use. All the other regents were of analytical grade and used as received.

2.2. Synthesis of octa(chloropropyl) POSS (OCPS)

OCPS [$(C_3H_6Cl)_8Si_8O_{12}$] was synthesized by following the method described by Jiang et al. [13] (Scheme 1). Typically, 1800 mL methanol, 79.5 g (0.4 mol) 3-chloropropyltrimethoxysilane, and 90 mL concentrated hydrochloric acid were mixed and the hydrolysis and rearrangement reactions were allowed to carry out for at least 5 weeks and 19.3 g (yield: 42.1%) colorless crystals were obtained after dried in vacuo at 80 °C for 24 h.

FTIR (KBr, cm^{-1}): 2984, 2954, 2872 (ν_{C-H}); 1109 ($\nu_{Si-O-Si}$), 759 (ν_{C-Cl}).

^1H NMR ($CDCl_3$, δ, ppm, TMS): 3.54 (m, 2H, $SiCH_2CH_2CH_2Cl$,); 1.88 (m, 2H, $SiCH_2CH_2CH_2Cl$); 0.83 (m, 2H, $SiCH_2CH_2CH_2Cl$,) (Fig. 1, A).

^{29}Si NMR ($CDCl_3$, δ, ppm): −67.03 ($Si-CH_2-$) (Fig. 1, B).

2.3. Synthesis of octa(azidopropyl) POSS (OAPS)

OCPS [$(C_3H_6Cl)_8Si_8O_{12}$] (1.0 g, 1.0 mmol) and 15 mL of DMF were added into a round bottom flask. Sodium azide (0.78 g, 12.0 mmol) was added to the solution. The reaction was kept for 60 h at 70 °C (Scheme 1). Then deionized water was added into the reaction mixture to wash NaN_3, and ethyl acetate was added to extract the product. The ethyl acetate solution was subjected to rotary evaporation to obtain colorless liquid with high viscosity and dried in a vacuum oven for 12 h at 80 °C.

FTIR (KBr, cm^{-1}): 2984, 2954, 2872 (ν_{C-H}); 1109 ($\nu_{Si-O-Si}$), 2100 (ν_{C-N3}).

^1H NMR ($CDCl_3$, δ, ppm, TMS): 3.31 (m, 2H, $SiCH_2CH_2CH_2N_3$); 1.68 (m, 2H, $SiCH_2CH_2CH_2$ N_3); 0.72 (m, 2H, $SiCH_2CH_2CH_2$ N_3) (Fig. 1,A).

^{29}Si NMR ($CDCl_3$, δ, ppm): −68.37 ($Si-CH_2-$) (Fig. 1,B).

Elemental analysis for $(N_3C_3H_6)_8Si_8O_{12}$, found (calcd) (%): N: 31.73 (32.81), C: 27.90 (28.13), H: 4.67 (4.69).

^{29}Si NMR and ^1H NMR resonance integration shows that eight chlorine groups of octa(chloropropyl) POSS (OCPS) were totally changed into N_3 groups in azido substitution step.

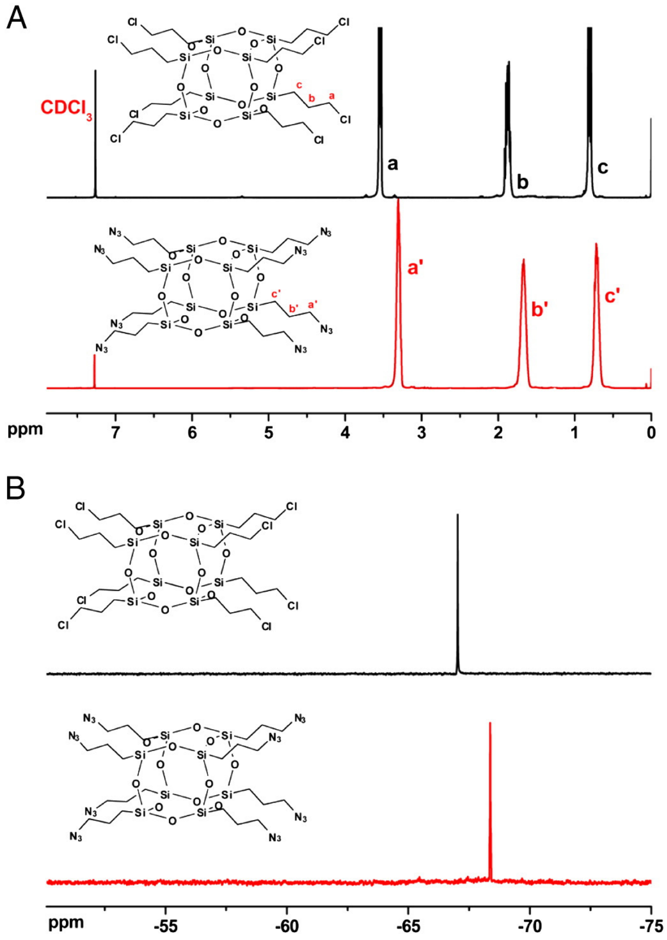

Fig. 1. NMR spectrum of OAPS. A. ^1H NMR spectra, B. ^{29}Si NMR spectra.

2.4. Synthesis of propargyl-terminated PEO

Propargyl-terminated PEO was synthesized by following the method described by Ke Zeng et al. [14] (Scheme 1). Prior to use, the PEO samples (M_n 5000) were dried via azeotropic distillation with toluene. In a typical experiment, to a 500 mL round bottom flask, NaH (0.96 g, 40 mmol) and anhydrous THF (50 mL), PEG (M_n 5000) (20.0 g) dissolved in 150 mL anhydrous THF was slowly added dropwise to the system within 30 min. The mixture was maintained at 30 °C for 3 h and then propargyl bromide (2.38 g, 20 mmol) dissolved in 50 mL

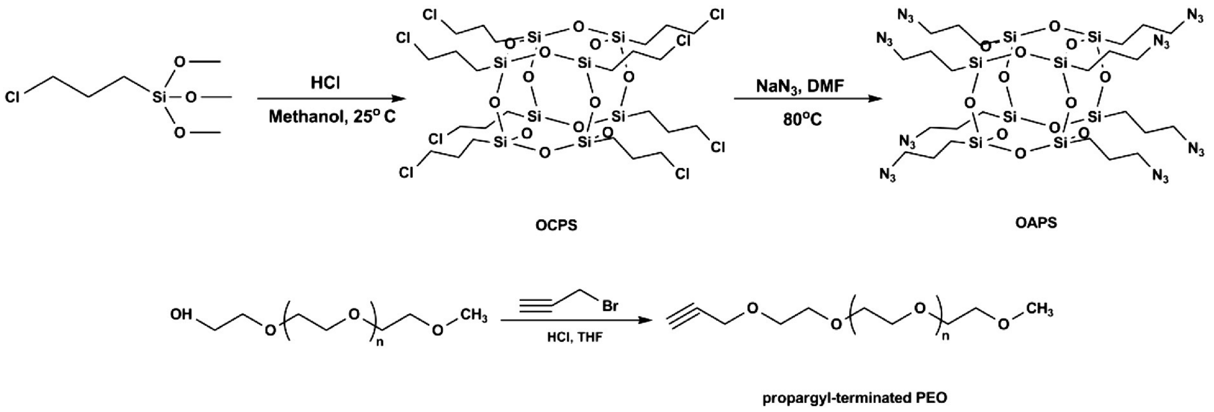

Scheme 1. Preparation of OAPS and propargyl-terminated PEO.

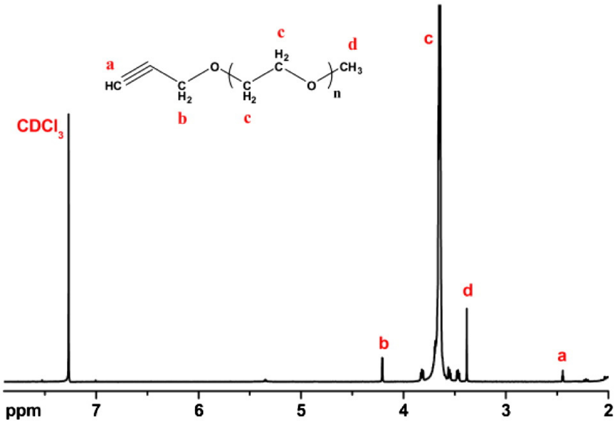

Fig. 2. ^{1}H NMR spectrum of propargyl-terminated PEO ($M_n = 5000$).

anhydrous THF was added dropwise. The reaction was carried out for a further 20 h with vigorous stirring to reach completion. The salt (i.e., NaBr) and the unreacted NaH were removed by filtration. The filtrate was concentrated and precipitated in a large amount of petroleum ether. The precipitates were dissolved in THF and re-precipitated with petroleum ether. This procedure was repeated three times to purify the products. The product was dried in vacuo at 30 °C for 24 h. The product, propargyl-terminated PEO (19.95 g), was obtained at a yield of 93%.

FTIR (KBr, cm^{-1}): 243 ($H-C\equiv$), 2106 ($-C\equiv C-$).

^{1}H NMR ($CDCl_3$, δ, ppm, TMS, PEG, Mn: 5000): 2.44 (t, 1.0H, $HC\equiv C$), 4.23 (d, 1.6H, $-C\equiv C-CH_2-$), 3.62 (m, 391.8H, $-CH_2-CH_2-O$), 3.41 (s, 2.8H, CH_3-O-). (Fig. 2)

2.5. Synthesis of OAPS–PEO via “Click” chemistry

The OAPS–PEO was synthesized via “click” reaction as shown in Fig. 3. OAPS (0.10 g, 0.10 mmol) and propargyl-terminated PEO (5.0 g, 1.0 mmol) were dissolved in THF (20.4 g, 20%wt), and then $CuSO_4$ (2.6 mg, 0.016 mmol) and sodium ascorbate (6.3 mg, 0.032 mmol) were added. The reaction was maintained at 70 °C for 24 h to reach completion.

2.6. Preparation of micelles

OAPS–PEO was first dissolved in a small volume of THF, followed by the slow addition (1 mL/min) of a known volume of water. An example is given for the preparation of 1.0 mg/mL of OAPS–PEO in aqueous solution. Polymer (2.0 mg) was dissolved in THF (0.5 mL), and the solution was diluted with deionized water (2.0 mL). To follow the THF evaporation from solution, the mass of the initial polymer solution (2.5 mL) was measured. Next, the solution was left to evaporate at room temperature until the volume dropped to the 2.0 mL level, and the mass was observed to decrease until it remained constant (~12 h). The drop in the volume and mass of the solution could be mainly due to the evaporation of THF (0.5 mL of THF was added to dissolve the polymer) as the rate of evaporation of THF is much faster as compared with water at room temperature. Before analysis, the solutions were stabilized for at least 5 days.

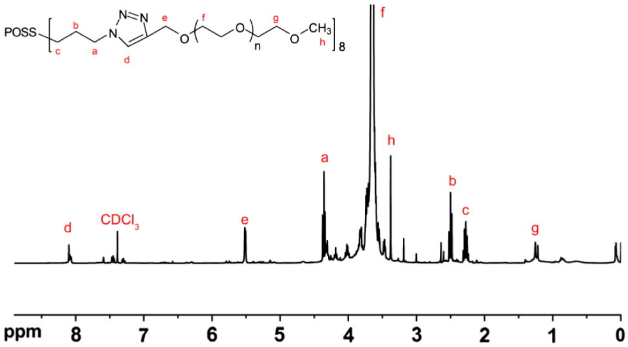

Fig. 4. ^{1}H NMR spectra of OAPS–PEG from propargyl-terminated PEO ($M_n = 5000$).

2.7. Characterization

2.7.1. Transmission electron microscopy (TEM)

The morphologies of the aggregates were examined by TEM (JEM-1400, JEOL) operated at an accelerating voltage of 120 kV. Drops of solution were placed on a copper grid coated with carbon film and then were dried at room temperature.

2.7.2. Laser light scattering (LLS) measurements

LLS was measured by an LLS spectrometer (ALV/CGS-5022F) equipped with an ALV-High QE APD detector and an ALV-5000 digital correlator using a He–Ne laser (the wavelength $\lambda = 632.8$ nm) as the light source. All the samples were filtered through 0.8 μm filters, and the measurements were carried out at 20 °C.

In static LLS, the angular dependence of the excess absolute time-average scattered intensity, i.e. Rayleigh ratio $R_{vv}(q)$ of the dilute polymer solutions was measured. $R_{vv}(q)$ is related to the weight-average molar mass (M_w), polymer concentration (C), and the scattering angle (φ) as

$$KC/R(\varphi, C) = 1/M_w\left[1+\left(R_g{}^2q^2\right)/3\right]+2A_2C$$

where $K = 4\pi^2 n^2 (dn/dC)^2/(N_A\lambda^4)$ and $q = 4\pi n \sin(\varphi/2)/\lambda$ with N_A, dn/dC, n, and λ being the Avogadro number, the specific refractive index increment, the solvent refractive index, and the wavelength of

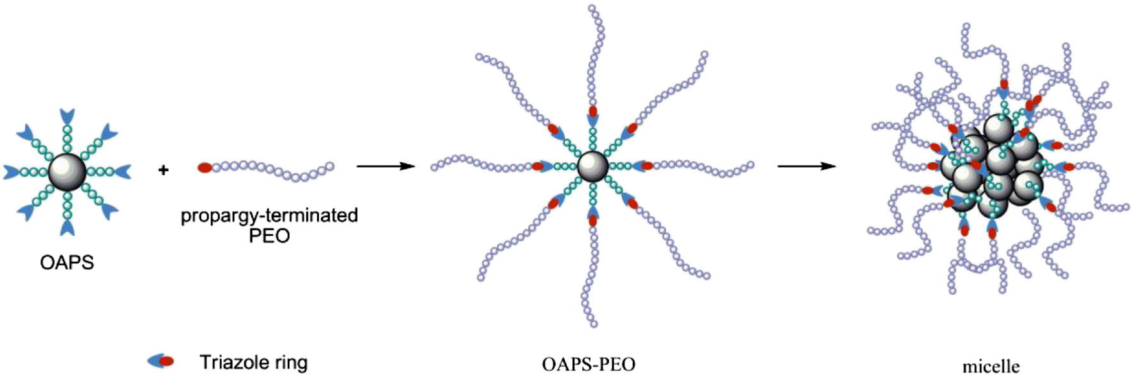

Fig. 3. Preparation of amphiphilic OAPS–PEO.

Table 1
GPC results of OAPS, PEO and OAPS–PEO.

	M_n	M_w	M_w/M_n
OAPS	4802	5728	1.19
PEO	5000	5048	1.05
OAPS–PEO	24,969	28,121	1.13

the light in vacuum, respectively; A_2 is the second virial coefficient, and R_g is the z-average radius of gyration of the aggregates in solution. By extrapolating to zero concentration and zero angle, R_g values of the aggregates can be calculated.

In dynamic LLS measurement, the Laplace inversion of each measured intensity–intensity time correlation function $G^{(2)}(t,q)$ in the self-beating mode can result in a line width distribution $G(\Gamma)$. The translational diffusion coefficient D calculated from the decay time, Γ, by the slope of the Γ versus q^2 plot, can lead to hydrodynamic radius R_h by the Stokes–Einstein equation $R_h = k_BT/(6\pi\eta D)$, where k_B, T, and η are the Boltzmann constant, the absolute temperature, and the solvent viscosity, respectively.

3. Results and discussion

Due to advantages of the "click" reaction with high yield, nearly eight PEO chains linked with OAPS. Fig. 4 shows ^{1}H NMR spectra of the amphiphilic OAPS–PEO. The resonance at $\delta = 8.10$ ppm is attributed to the protons of triazole structures resulting from the click reaction. The ^{1}H NMR spectra indicate that amphiphilic OAPS–PEO was successfully obtained. Methylene protons of OAPS at $\delta = 3.31, 1.68, 0.72$ ppm are all shifted to $\delta = 4.36, 2.50, 2.27$ ppm, respectively. The disappearance of the peaks for the methylene groups at 0.72 ppm, 1.68 ppm and 3.31 ppm of OAPS in ^{1}H NMR spectra of OAPS–PEO indicates that N_3 groups were well reacted.

The GPC result of OAPS–PEO reveals the increase in molecular weight obtained by the triazole ring of PEO with OAPS. The M_n, M_w, and the molecular weight distribution (M_w/M_n) are listed in Table 1. It indicates that approximately five PEO chains were attached to the OAPS core. This result is lower than the theoretically expected value for OAPS, with ~8 PEO chains estimated from the ^{1}H NMR result. It is not surprising that OAPS–PEO has a spherical micelle structure while the standard PEG is a linear chain, as star polymers typically possess smaller hydrodynamic volumes. Nevertheless, a relatively narrow and unimodal distribution ($M_w/M_n = 1.13$) of OAPS–PEO confirms the successful synthesis of OAPS–PEO. As we know, it is difficult to obtain the complete substitution of octafunctional cubic silsesquioxane in other literatures [12], thus, the "click" reaction could probably be an efficient way to prepare octasubstitution cubic silsesquioxane.

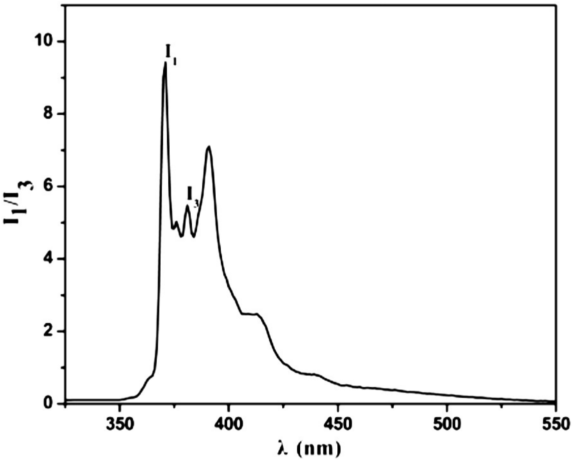

Fig. 5. Fluorescence spectra of OAPS–PEG. (Probe:pyrene).

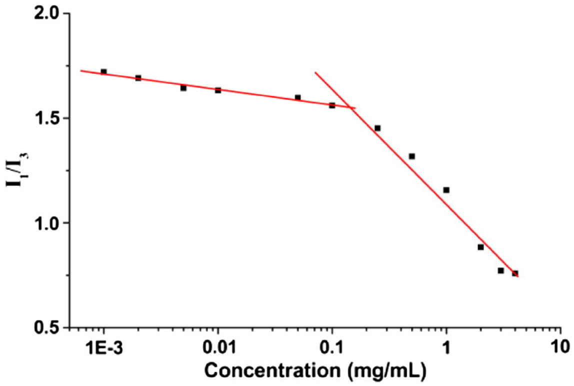

Fig. 6. Variation of the intensity ratio (I_1/I_3) as a function of OAPS–PEO concentration.

The aggregates behavior of OAPS–PEO in aqueous solution was investigated by fluorescence measurement using pyrene as a probe. This method has been widely used to determine the aggregate process of amphiphilic polymers in aqueous solution [14]. I_1 and I_3 stand for the first and the third vibronic peak intensities (Fig. 5). The intensity ratio of I_1 to I_3 of pyrene decreases with the decline of polarity of solutions. At low concentrations, OAPS hydrophobic domains are so small that pyrene molecules are mainly solubilized in the aqueous phase. When aggregates occur by the addition of water, large hydrophobic domains are formed within the aggregates, and the pyrene preferentially penetrates into the hydrophobic core. The critical aggregate concentration (CAC) is identified by the inflection point in plot of I_1/I_3 versus concentration, which is determined to be ~0.1 mg/mL (Fig. 6).

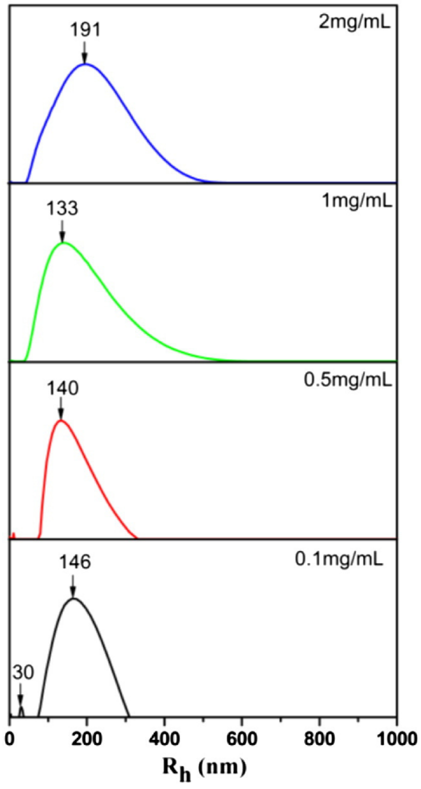

Fig. 7. Concentration dependence of hydrodynamic radius distribution functions of OAPS–PEO. (Bottom to top: 0.10, 0.50, 1.0 and 2.0 mg/mL).

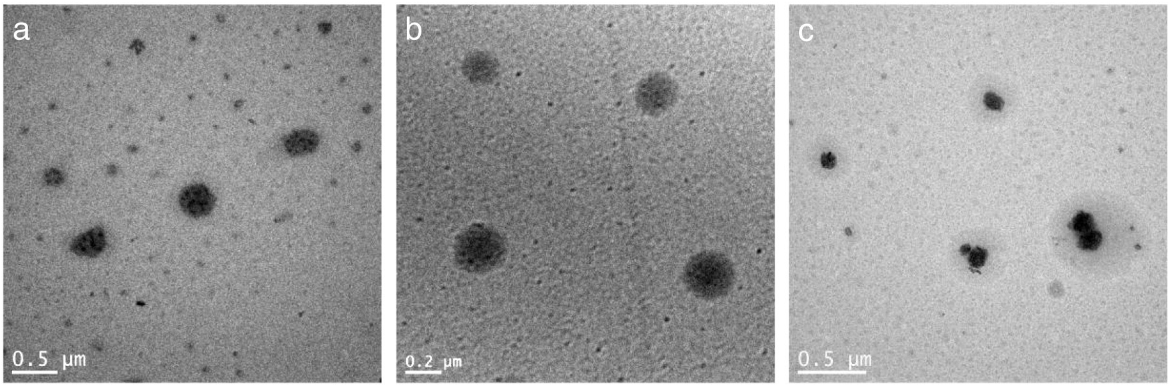

Fig. 8. Transmission electron micrographs of OAPS–PEO at different concentrations: (a) 0.10 mg/mL, (b) 0.50 mg/mL, and (c) 2.0 mg/mL.

Table 2
Static and dynamic light scattering studies of OAPS–PEO in water at 25 °C.

Concentration (mg/mL)	R_g (nm)	R_h (nm)	R_g/R_h
0.10	110	101	1.09
0.25	140	140	1.00
0.50	154	146	1.06
1.0	183	133	1.38
2.0	287	190	1.51

The hydrodynamic properties and aggregation behavior of OAPS–PEO in aqueous solution were also investigated by dynamic and static light scattering studies. Fig. 7 shows the size distribution of OAPS–PEO at different concentrations measured at 90°. The peaks attributed to the scattering from the large particles are attributable to the aggregates of OAPS–PEO. The aggregates peak is observed, even at a concentration of 0.1 mg/mL, which is in agreement with the fluorescence measurements (CAC) ~0.1 mg/mL. Two size distribution peaks are observed at concentrations of 0.1 mg/mL, although the scattered intensity of the first peak is very weak about 10%. The small peak represents the unassociated unimolecular micelle with $R_h = \sim 30$ nm and the dominant peaks attributed to the scattering from the large particles attributable to the aggregation of OAPS–PEO. Fig. 8a shows the TEM micrographs of OAPS–PEO at the concentration of 0.10 mg/mL. Unassociated unimolecular micelles in the range of 40–50 nm can be seen in this picture. The end-to-end distance of PEO with the size of the OAPS cage was calculated according to the literature assuming a helical configuration of PEO [15] and found to be ~36 nm. The value of R_h for OAPS–PEO unassociated unimolecular micelles is larger than the end-to-end distance of OAPS–PEO while DLS gives the R_h in aqueous solution. Below the concentration of 0.50 mg/mL, R_g/R_h is found to be ~1.06 (Table 2), which is reported to be the ratio of star polymer with many arms [16]. It is also consistent with the picture of the aggregates in Fig. 8a and b. At a larger concentration higher than 1 mg/mL, the ratio of R_g/R_h has obviously ascent. It is illuminating that the aggregates of OAPS–PEO amphiphilic are turned to be another form, which has hard spheres surrounded by loose shell. It means OAPSs concentrate to be a core, and PEO arms which have greater thermodynamic penetrability are in the outer layer of the OAPS–PEO aggregates (Fig. 8c). K. Yi Mya and co-workers [12] described the R_g/R_h value for core–shell structures.

The conformations of the aggregates at different concentrations can be schematically illustrated as shown in Fig. 9. At the concentration about CAC, there exists the unassociated unimolecular micelle. By the concentration ascending, the OAPS–PEO amphiphilics are aggregating to be loose balls, and turning to be core–shell like micelle at the concentration of 2.0 mg/mL. The micelle may have application in drug delivery and other fields.

4. Conclusions

Octa(azidopropyl) POSS was prepared and attached with propargyl-terminated PEO to synthesize the amphiphilic OAPS–PEO. The critical aggregation concentration was determined to be ~0.1 mg/mL by using fluorescence measurements. At this concentration, unassociated unimolecular micelles with a size of 30–40 nm in diameter were found by DLS and TEM. With the increase of OAPS–PEO concentration, R_g/R_h also ascends. At the concentration of 2.0 mg/mL, the aggregation presents to be a core–shell structure with R_g/R_h of 1.51.

Acknowledgment

The authors gratefully acknowledge the financial support of Shanghai Leading Academic Discipline Project (B502) and Fundamental Research Funds for the Central University (WD113006).

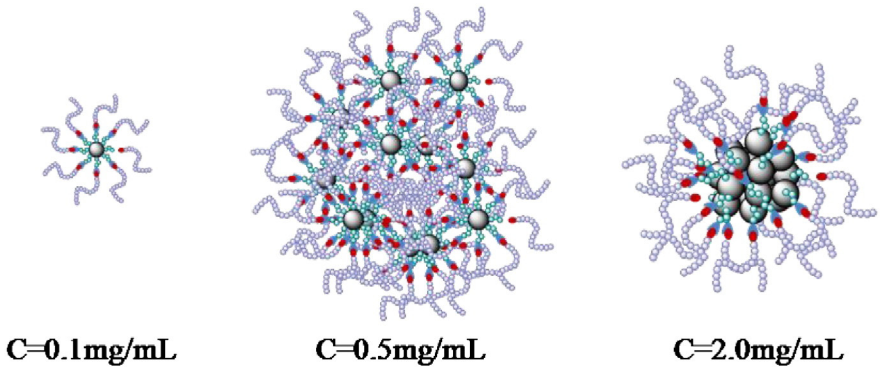

Fig. 9. Schematic representation of OAPS–PEO aggregates formation at different concentrations: 0.10, 0.50 and 2.0 mg/mL.

References

[1] M.M. Sprung, F.O. Guenther, J. Am. Chem. Soc. 77 (1955) 3990.
[2] J.F. Brown, J. Am. Chem. Soc. 87 (1965) 4317.
[3] K. Pielichowski, J. Njuguna, B. Janowski, J. Adv. Polym. Sci. 201 (2006) 225.
[4] R.M. Laine, J. Mater. Chem. 15 (2005) 3725.
[5] J. Wu, P.T. Mather, Macromol. Sci. Polym. Rev. 49 (2009) 25.
[6] R. Knischka, F. Dietsche, R. Hanselmann, H. Frey, R. Mülhaupt, Langmuir 15 (1999) 4752.
[7] P. Maitra, S.L. Wunder, Chem. Mater. 14 (2002) 4494.
[8] B.S. Kim, P.T. Mather, Macromolecules 35 (2002) 8378.
[9] H. Li, J. Sun, A. Qin, B.Z. Tang, Chin. J. Polym. Sci. 30 (2012) 1.
[10] H. Chow, K. Lau, M. Chan, Chem. Eur. J. 17 (2011) 8395.
[11] Z.S. Ge, D. Wang, Y.M. Zhou, H.W. Liu, S.Y. Liu, Macromolecules 42 (2009) 2903.
[12] K.Y. Mya, X. Li, L. Chen, X.P. Ni, J. Li, C.B. He, J. Phys. Chem. B 109 (2005) 9455.
[13] Z.Y. Jiang, Y. Zhou, F.R. Huang, L. Du, Chin. J. Polym. Sci. 29 (2011) 726.
[14] A.P. Narrainen, S. Pascual, D.M. Haddleton, J. Polym. Sci. A Polym. Chem. 40 (2002) 439.
[15] J.A. Johnson, M.L. Saboungi, D.L. Price, S.J. Ansell, Chem. Phys. 109 (1998) 7005.
[16] W. Burchard, M. Schmidt, W.H. Stockmayer, Macromolecules 13 (1980) 1265.